KnE Materials Science

ASRTU Conference on Alternative Energy
Sino-Russian ASRTU Conference Alternative Energy: Materials, Technologies, and Devices
Volume 2018

Knowledge E
Engaging minds

Conference Paper

Thermal Performance Analysis of High-temperature Heat Transfer Process of Solar Energy

X. L. Xia[1], F. X. Sun[2], H. P. Tan[1], and X. Chen[1]

[1]Key Laboratory of Aerospace Thermophysics of MIIT, Harbin Institute of Technology, Harbin 15001, China
[2]School of Power and Energy Engineering, Harbin Engineering University, Harbin 15001, China

Abstract

Volumetric solar receivers (VSR) have become a promising technology for the solar thermal conversion. The absorption of the concentrated solar radiation and the heat transfer to the working fluid are the two dominant processes. Firstly, the effects of two typical modeling approaches of the concentrated solar radiation for receiver are compared in view of porosity and mean cell size. Then, the radiation transport within the solar window and the porous absorber is fully simulated. The effects of porous structure parameters, slope error of the concentrator, and the alignment error of the receiver are analyzed.

Keywords: volumetric solar receivers (VSR), Monte Carlo ray tracing method, concentrated solar radiation, heat transfer

Corresponding Author:
X. L. Xia
xiaxl@hit.edu.cn

Received: 14 September 2018
Accepted: 1 October 2018
Published: 14 October 2018

Publishing services provided by Knowledge E

Selection and Peer-review under the responsibility of the ASRTU Conference Committee.

1. Introduction

Volumetric receiver with high-porosity material appears to be a promising technology for converting solar flux into thermal energy [1]. As one of the most important heat transfer processes in the receiver, the solar radiation transmission and absorption process is important to the overall system performance [2]. The thermal behavior and efficiency of the solar receiver have been extensively investigated. The incoming concentrated solar radiation is modeled using two major approaches. In the first approach, the heat flux at the boundary is considered as a surface phenomenon based on the assumption of very large optical thickness for the porous media. The solar flux distribution is treated as the secondary type thermal barrier coating (TBC) in the simulation [3]. This assumption neglects the gradual absorption characteristics of the solar radiation in the receiver and cannot reflect the volumetric effect.

The second approach incorporates the solar radiation transport within the volumetric receiver, and the concentrated solar radiation is considered as a radiative heat source in the whole volume of receiver [4]. Nevertheless, instead of appropriate modeling, the concentrated solar flux distribution, the impinging solar radiation on the front surface of receiver has been treated as a Cox-Ingersoll-Ross (CIR) beam with a uniform or Gaussian distribution in several studies. In fact, the concentrated solar radiation is extremely nonuniform in spatiality and direction. This distribution has a significant impact on the temperature field in the solar receiver [5]. Therefore, the performance evaluation of the solar receiver should be based on the coupling between solar flux modeling and heat transfer modeling [6]. Monte Carlo Ray Tracing (MCRT) simulations have been carried out to obtain the realistic concentrated heat flux distribution boundary conditions by some researchers.

An integrated model of solar radiation propagation in a concentrator-window-absorber system is established. The local solar radiative source distribution within the porous absorber and the optical efficiency of the system are predicted with the MCRT method. The flow and heat transfer simulation of a solar receiver with double-layer ceramic foam is performed in this study. The effects of geometric parameters of each porous layer on the thermal performance are mainly discussed.

2. Methods

2.1. Model description

A key component in the solar thermal system is the volumetric receiver, which is located at the focal plane of the concentrator. As shown in Figure 1, the solar radiation is collected and redirected to the receiver by the dish concentrator. The surface equation for the dish is:

$$z = \frac{x^2 + y^2}{4f}, \tag{1}$$

where f is the focal length of the dish.

The optical errors may enlarge the solar image and reduce the optical performance of system [7]. For a solar concentrator, the sources of optical errors are typically a slope error σ_{slope}, a tracking error σ_{track}, a nonspecular reflection σ_{scatt}, and some alignment error σ_{align} [8]:

$$\sigma_{opt}^2 = (2\sigma_{slope})^2 + \sigma_{track}^2 + \sigma_{scatt}^2 + \sigma_{align}^2 \tag{2}$$

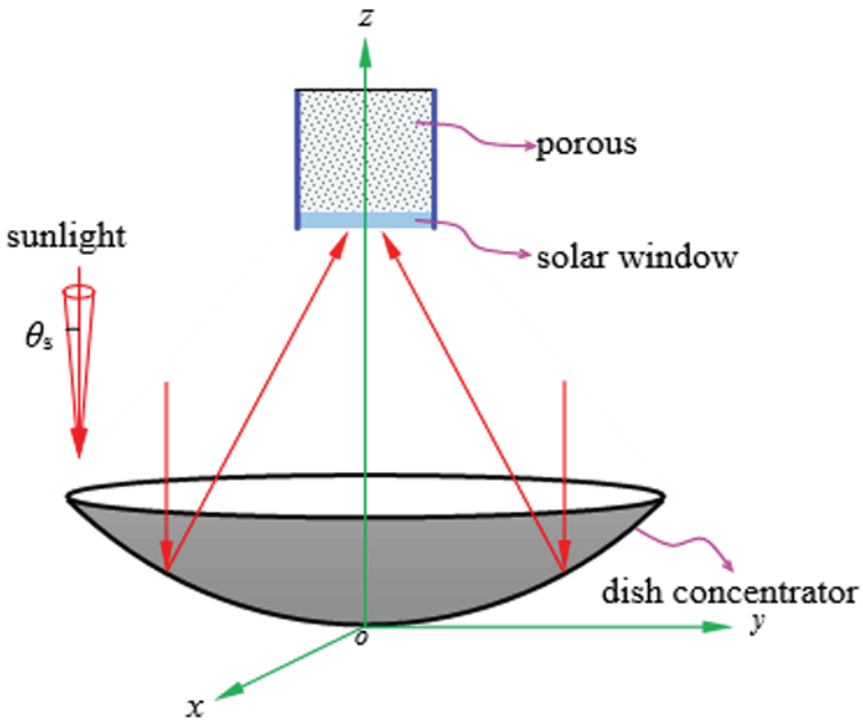

Figure 1: Schematic of the volumetric receiver with solar dish concentrator system.

The heat transfer model for numerical analysis is shown in Figure 2. A local cylindrical coordinate system *o*-rφz is established for the porous media. Besides, the reflection and absorption also occurs at the receiver wall. Geometrical and physical parameters of the concentrator and volumetric solar receiver are presented in Table 1.

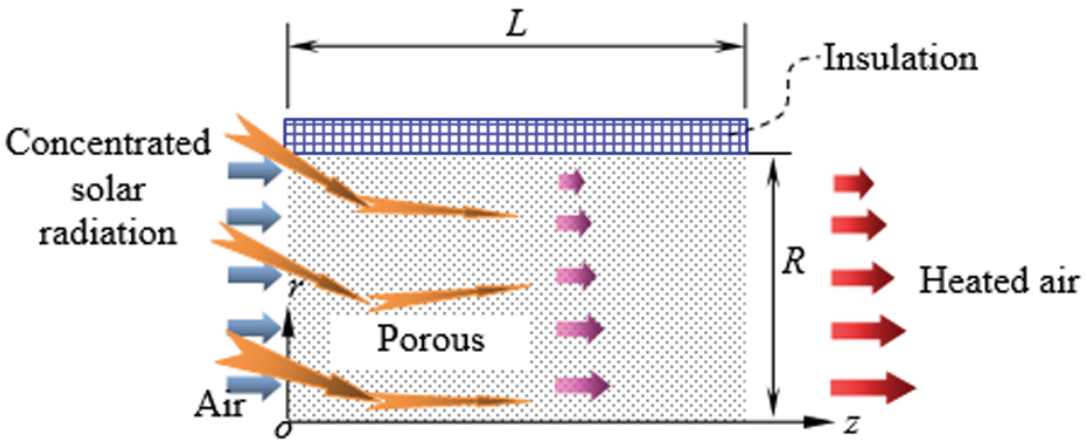

Figure 2: Schematic diagram of heat transfer in the volumetric solar receiver across a gray slab.

Table 1: Geometrical and physical parameters of the concentrator and volumetric solar receiver.

Concentrator and Volumetric Receiver	Value
Focal length of the dish concentrator (f)	3.25 m
Aperture radius of the dish concentrator (R_C)	1.3 m
Length of the porous media (L)	0.05 m
Diameter of the receiver ($2R$)	0.05 m
Thickness of the plane window (h_g)	8 mm
Distance between the window and the porous media (h_1)	5 mm
Refractive index of the window (n_g)	1.42
Absorption coefficient of the window (k_g)	1.4 m^{-1}
Emissivity of the porous media (ε)	0.92
Emissivity of the receiver wall (ε_w)	0.3
Reflectivity of the dish surface (ρ_C)	0.9
Slope error of the dish concentrator (σ_{slope})	2.0 mrad

2.2. Solar radiation transport simulation

MCRT method is a random simulation method based on the probability statistics and is widely used in concentrated solar research [9]. The pillbox distribution is chosen to describe the sunshape effect, which means that the solar radiation is constant within a cone with a half angle of $\theta_s = 4.65$mrad [10]. Besides, the value of the solar radiation heat flux incident on the concentrator used in this study is $q_s = 1000\text{W/m}^2$ [11]. The slope error σ_{slope} is applied to indicate the deviation of a real dish surface from a perfect one. In MCRT process, the slope deviation can be defined by a azimuth angle φ_{se} and a zenith angle θ_{se}, which can be determined by the following expressions [12]:

$$\theta_{se} = \sqrt{(-2\sigma_{slope}^2)\ln(1 - R_{s\theta})} \tag{3}$$

$$\varphi_{se} = 2\pi R_{s\varphi}, \tag{4}$$

where $R_{s\theta}$ and $R_{s\varphi}$ are random numbers, which are uniformly distributed between 0 and 1.

Once the ray penetrates into the porous media, based on media radiation transfer theory, a possible transfer distance may be obtained from the following probability expression [13]:

$$l_\beta = -\frac{1}{\beta}\ln R_\beta, \tag{5}$$

where β is the extinction coefficient and R_β is a random number, which ranges from 0 to 1 uniformly. When the location l_β is reached, the second random number R_ω is required to decide whether the ray is absorbed or scattered, with ω being the scattering albedo ($\omega = \sigma_s/\beta$, where σ_s is the scattering coefficient.) [14]:

$$\begin{aligned} R_\omega &\le \omega, \ \text{scattering} \\ R_\omega &> \omega, \ \text{absorption} \end{aligned} \tag{6}$$

If the ray is scattered, it will travel into a new direction. Otherwise, the ray is absorbed by the local element. The solar radiative source of the element *i* caused by the concentrated solar radiation can be computed as:

$$S_{sr,i} = \frac{N_i \cdot e}{\Delta V_i}, \tag{7}$$

where N_i denotes the number of rays absorbed within the volume element, ΔV_i is the volume of the element, which can be determined based on the element division, and e represents the energy carried by each ray sampling, $e = q_s/n_{ray}$, where n_{ray} is the ray sampling number per unit area.

2.3. Heat transfer simulation within the receiver

The governing equations are described as follows.

2.3.1. Continuity equation

$$\nabla \cdot \left(\rho_f \overrightarrow{V}\right) = 0, \tag{8}$$

where ρ_f is the fluid density and $\overrightarrow{V}$ denotes the superficial velocity.

2.3.2. Momentum equation

Flow in the porous media is modeled by adding a momentum source term to the standard fluid flow equation, which can be expressed as [4]:

$$\frac{1}{\phi}\nabla\left(\rho_f \frac{\overrightarrow{V}\cdot\overrightarrow{V}}{\phi}\right) = -\nabla p + \nabla\cdot\left(\frac{\mu_f}{\phi}\nabla\overrightarrow{V}\right) + \overrightarrow{F}, \tag{9}$$

where p is the pressure of fluid, μ_f is the dynamic viscosity, ϕ is the porosity, and $\vec{F}$ is the momentum source term to calculate the pressure drop resulting from the porous media, which is calculated by the following equation [15]:

$$\vec{F} = -\frac{1039 - 1002\phi}{d_c^2}\mu_f \vec{V} - \frac{0.5138\phi^{-5.739}}{d_c^2}\rho_f \left|\vec{V}\right| \vec{V}, \tag{10}$$

where d_c is the mean cell size. This equation is valid for $0.66 < \phi < 0.93$, $10 < Re < 400$ ($Re = \rho_f u d_c/\mu_f$) and a cross-section of the pore channel that approaches to a circle.

2.3.3. Energy equation

The energy equations with LTNE condition for the fluid phase and solid phase can be expressed as follows [16].

For the fluid phase:

$$\nabla \cdot \left(\rho_f c_p \vec{V} T_f\right) = \nabla \cdot \left(\lambda_{fe} \nabla T_f\right) + h_v(T_s - T_f). \tag{11}$$

For the solid phase:

$$0 = \nabla \cdot \left(\lambda_{se} \nabla T_s\right) + h_v(T_f - T_s) + S_r, \tag{12}$$

where T_f and T_s are the fluid and solid temperatures, respectively, c_p is the specific heat of fluid, S_r is the volumetric heat source term due to radiative heat transfer, and the effective thermal conductivity for the fluid phase and solid phase could be determined using the Schuetz–Glicksman empirical formulas [9]:

$$\lambda_{fe} = \phi\lambda_f \tag{13}$$

$$\lambda_{se} = \frac{1}{3}(1 - \phi)\lambda_s \tag{14}$$

The symbol h_v is the volumetric convection heat transfer coefficient between the fluid phase and the solid phase. The empirical correlation proposed by Wu et al. [17] is used:

$$h_v = \lambda_f(32.504\phi^{0.38} - 109.94\phi^{1.38} + 166.65\phi^{2.38} - 86.98\phi^{3.38})Re^{0.438}/d_c^2 \tag{15}$$

This correlation is valid for $0.66 < \phi < 0.93$ and $70 < Re < 800$.

2.3.4. Boundary conditions

The front surface of the porous media is subjected to the concentrated solar radiation. The boundary conditions are as follows:

$$x = 0 : T_f = 300K, \tag{16}$$

$$x = L : \partial T_f/\partial x = \partial T_f/\partial r = \partial T_s/\partial x = \partial T_s/\partial r = 0, \quad (17)$$

$$x = 0 : u = u_{in}, v = 0, \quad (18)$$

$$x = L : \partial u/\partial x = \partial u/\partial r = \partial v/\partial x = \partial v/\partial r = 0. \quad (19)$$

2.4. Thermophysical parameters

The porous media is assumed to be SiC foam with isotropic properties. The thermal properties are assumed to be constant. The thermal conductivity is 80 W/(m·K). The thermal capacity and density of bulk SiC are 750 J/(kg·K) and 3200 kg/m^3, respectively [4]. Air is regarded as ideal gas and the viscosity is calculated through Sutherland Law. The thermal capacity and conductivity can be described as functions of temperature by the following polynomial functions [15]:

$$c_p = 1.93 \times 10^{-10} T_f^4 - 8 \times 10^{-7} T_f^3 + 1.14 \times 10^{-3} T_f^2 - 4.49 \times 10^{-1} T_f + 1.06 \times 10^3 \quad (20)$$

$$\lambda_f = 1.52 \times 10^{-11} T_f^3 - 4.86 \times 10^{-8} T_f^2 + 1.02 \times 10^{-4} T_f - 3.93 \times 10^{-3} \quad (21)$$

3. Results

3.1. MCRT model validation

To examine the validity of the numerical simulation, two comparative studies have been carried out. First, for the solar flux modeling, the solar flux distributions at the focal plane for two dish concentrators with the case of $f = 5.0$ m at $\sigma_{slope} = 2.0$ mrad are simulated. The results are compared with the data obtained by Lee et al. [18], where ψ_{rim} is the rim angle. To further validate the radiative transfer simulation using the P1 approximation, the results are compared with those in [14].

3.2. Heat transfer results of receiver

3.2.1. Effects of porous structure parameters

The porosity and pore diameter are the two main parameters to characterize the porous structure. The impacts of porosity and pore diameter on the receiver performance are studied, respectively. A local coordinate system *O-XYZ* is aligned with the porous absorber, where the *XY* plane is set on the bottom surface of the absorber.

According to the simulation, it can be seen that the radiative source decreases steeply along the center line and the maximum value decreases with the porosity increasing. The optical performance can be evaluated for different porosities, as illustrated in Table 2.

Table 2: Optical performance of the solar system with different porosities.

ϕ	η_{opt} (%)	η_{sw} (%)	η_{bs} (%)	η_{con} (%)
0.7	72.35	7.12	10.53	10.0
0.8	72.35	7.12	10.53	10.0
0.9	72.36	7.12	10.52	10.0
0.95	72.34	7.12	10.54	10.0

On the other hand, the extinction coefficient decreases with an increase in the pore diameter. The optical performance with different pore diameters is given in Table 3. The optical efficiency and optical losses have no noticeable change for different pore diameters. Besides, the structure parameters affect the distribution of absorbed solar energy within the absorber greatly and have no strong effect on the optical efficiency and optical losses.

Table 3: Optical performance of the solar system with different pore diameters.

d_p (mm)	η_{opt}(%)	η_{sw}(%)	η_{bs}(%)	η_{con}(%)
1.5	72.35	7.12	10.53	10.0
2.0	72.36	7.12	10.52	10.0
2.5	72.37	7.12	10.51	10.0
3.0	72.37	7.12	10.51	10.0

3.2.2. Effects of slope error of the solar concentrator

Slope error of the concentrator is a crucial factor in determining the concentrated solar flux and direction distribution affecting the receiver aperture. Figure 3 exhibits the effects of slope error on the distribution of solar radiative source and the optical performance. The optical efficiency decreases as the slope error increases, while the optical loss of dish concentrator increases gradually from 10.0% to 58.55%. The optical efficiency is 72.36% for $\sigma_{slope} = 0$ mrad, while it is 31.62% for $\sigma_{slope} = 3.0$ mrad.

3.3. Simulation methods

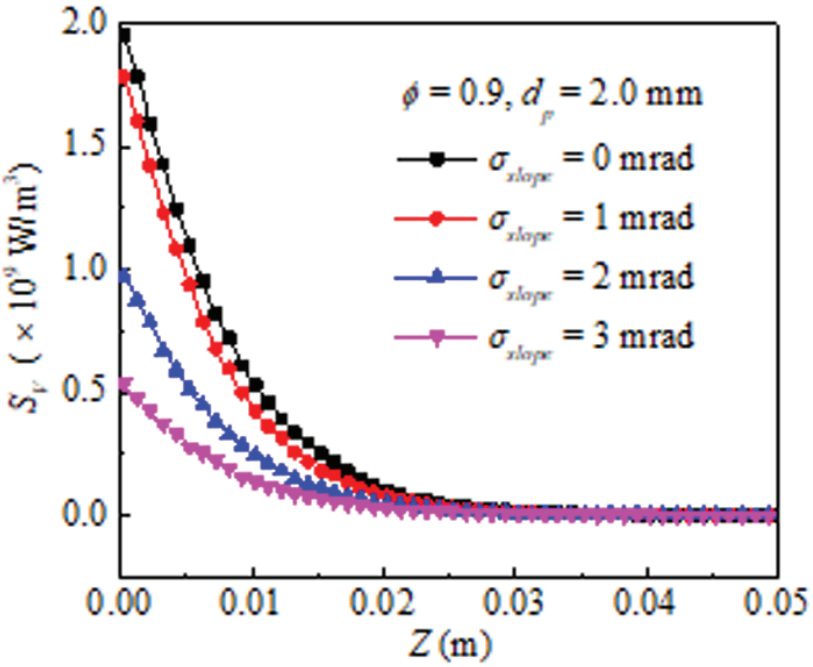

Figure 3: Distribution of the solar radiative source along the center line of porous absorber with different slope errors.

3.3.1. Comparison with the approach using TBC

To solve the conservation equations, FLUENT software with user defined functions is used implementing a two-dimensional axisymmetric model. The inlet velocity is set to 1.5 m/s. In this section, the TBC approach stating that the concentrated solar radiation is considered as thermal boundary condition is discussed.

The maximum temperature occurs at the front surface and the solid temperature decreases along the *z*-axis direction with the TBC approach. Since the extinction coefficient decreases reversely with the porosity, solar radiation can penetrate into the receiver much deeper with a high porosity. Besides, the heat absorbed in the front region is removed by convection effectively [19]. These factors result in the temperature distribution. The simplified TBC approach neglects the penetration of solar radiation into the receiver. This approximation may be suitable for a very low porosity with small mean cell size, since the extinction coefficient is extremely large. Thus, this TBC approach is not appropriate for predicting the temperature distribution in the receiver, especially in the front region.

3.3.2. Comparison with the approach using CIR

The corresponding percent distribution of incident solar radiation on the front surface along the zenith angle θ is presented in Figure 4. It can be seen that the maximum incident angle is about 23°, which contrasts with the approximation of collimated incidence. The absorbed solar radiation becomes concentrative in the center area near the front surface, and then the direction is redistributed due to the scattering of the porous media. Since isotropic scattering is considered, equal amounts of energy are scattered into all directions. As a result, the temperature away from the front surface shows no discernible difference between the two approaches. Therefore, the CIR approach can get acceptable results compared to the coupling simulation.

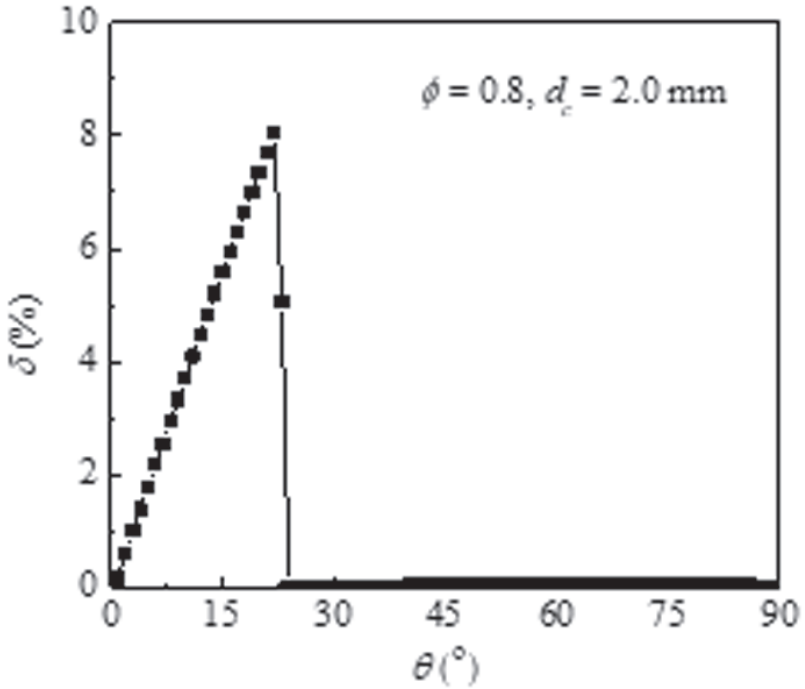

Figure 4: Directional characteristics of incident solar radiation on the front surface of the porous receiver.

3.3.3. Effects of slope error on the thermal performance

For a solar concentrator, the concentrating performance is significantly affected by the optical errors. The sources of optical errors are typically a slope error, a tracking error, nonspecular reflection, and some alignment error [8]. The predominant one is the slope error ranging from 1 to 6 mrad [8]. The previous studies mostly focus on the effects of characteristic parameters of the receiver on the thermal performance, whereas the effect of concentrating performance is excluded. Slope error

mainly causes the reflected ray to deviate from the specular reflection direction and eventually from the receiver. Figure 5 demonstrates that the slope error has a great influence on the temperature distribution.

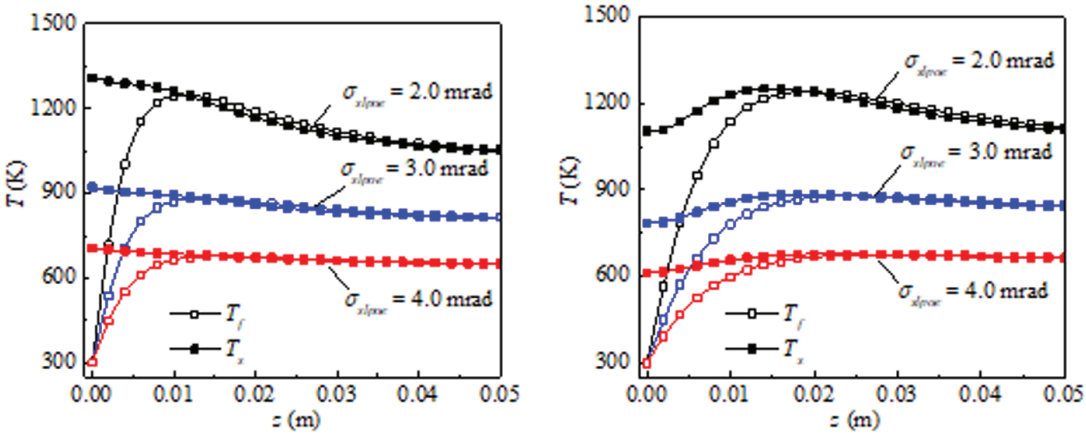

Figure 5: Effect of the slope error on the temperature distribution: (a) $\phi = 0.8$, $d_c = 2.0$mm (b) $\phi = 0.9$, $d_c = 2.0$mm.

4. Conclusion

In this study, a numerical model of volumetric solar receiver is presented by coupling the solar flux modeling and heat transfer modeling. As the first step, the solar radiation transport from concentrator to the interior of receiver is simulated with the MCRT method. The following conclusions have been drawn:

1. With the porosity increasing, the maximum radiative source within the porous absorber decreases and the distribution becomes uniform gradually. Moreover, the effect of porosity on the optical efficiency and losses is negligible. The effects of pore diameter on the solar radiative source and optical performance are similar to those of porosity.

2. The TBC approach obviously overestimates the solid temperature in the front region of receiver, while the outlet air temperature is underestimated. The temperature deviation increases as the porosity or mean cell size increases. The deviations of inlet solid and outlet air temperatures are up to 76.4% and 13.2%, respectively.

3. Using the CIR approach, the temperature distribution is almost the same as the result of coupling simulation except that the solid temperature near the front surface of receiver is slightly underestimated. The maximum deviation in this study is an acceptable value of 3.4%.

4. The slope error of solar concentrator has a remarkable influence on the temperature field in receiver. The fluid and solid temperatures both greatly decrease as the slope error increases. For example, the outlet air temperature decreases from 1053.9 K to 651.2 K as the slope error increases from 2.0 to 4.0 mrad for $\phi = 0.8$ and $d_c = 2.0$mm.

Funding

These investigations are supported by the National Natural Science Foundation of China (No. 51536001) and the Fundamental Research Project of China Industrial and Information Ministry (No. B2320132001).

References

[1] Roldán, M. I., Zarza, E., and Casas, J. L. (2015). Modelling and testing of a solar-receiver system applied to high-temperature processes. *Renewable Energy*, vol. 76, pp. 608–618.

[2] Cui, F. Q., He, Y. L., Cheng, Z. D., et al. (2012). Numerical simulations of the solar transmission process for a pressurized volumetric receiver. *Energy*, vol. 46, no. 1, pp. 618–628.

[3] Wang, F. Q., Shuai, Y., Tan, H. P., et al. (2013). Heat transfer analyses of porous media receiver with multi-dish collector by coupling MCRT and FVM method. *Solar Energy*, vol. 93, pp. 158–168.

[4] Villafán-Vidales, H. I., Abanades, S., Caliot, C., et al. (2011). Heat transfer simulation in a thermochemical solar reactor based on a volumetric porous receiver. *Applied Thermal Engineering*, vol. 31, no. 16, pp. 3377–3386.

[5] Wang, F. Q., Shuai, Y., Tan, H. P., et al. (2013). Thermal performance analysis of porous media receiver with concentrated solar irradiation. *International Journal of Heat and Mass Transfer*, vol. 62, pp. 247–254.

[6] Lee, H. J., Kim, J. K., Lee, S. N., et al. (2012). Consistent heat transfer analysis for performance evaluation of multichannel solar absorbers. *Solar Energy*, vol. 86, no. 5, pp. 1576–1585.

[7] Shuai, Y., Xia, X. L., and Tan, H. P. (2008). Radiation performance of dish solar concentrator/cavity receiver systems. *Solar Energy*, vol. 82, no. 1, pp. 13–21.

[8] Buie, D., Dey, C. J., and Bosi, S. (2003). The effective size of the solar cone for solar concentrating systems. *Solar Energy*, vol. 74, no. 5, pp. 417–427.

[9] Delatorre, J., Baud, G., and Bézian, J. J. (2014). Monte Carlo advances and concentrated solar applications. *Solar Energy*, vol. 103, pp. 653–681.

[10] Hasuike, H., Yoshizawa, Y., Suzuki, A., et al. (2006). Study on design of molten salt solar receivers for beam-down solar concentrator. *Solar Energy*, vol. 80, no. 10, pp. 1255–1262.

[11] Johnston, G. (1998). Focal region measurements of the 20m^2 tiled dish at the Australian National University. *Solar Energy*, vol. 63, no. 2, pp. 117–124.

[12] Dai, G. L., Xia, X. L., Sun, C., et al. (2011). Numerical investigation of the solar concentrating characteristics of 3D CPC and CPC-DC. *Solar Energy*, vol. 85, no. 11, pp. 2833–2842.

[13] Modest, M. F. (2013). *Radiative Heat Transfer* (third edition). San Diego: Academic Press.

[14] Vafai, K. (2005). *Handbook of Porous Media* (second edition). Porland: Taylor and Francis.

[15] Wu, Z. Y., Caliot, C., Flamant, G., et al. (2011). Coupled radiation and flow modeling in ceramic foam volumetric solar air receivers. *Solar Energy*, vol. 85, pp. 2374–2385.

[16] Wang, F. Q., Tan, J. Y., Ma, L. X., et al. (2014). Thermal performance analysis of porous medium solar receiver with quartz window to minimize heat flux gradient. *Solar Energy*, vol. 108, pp. 348–359.

[17] Wu, Z. Y., Caliot, C., Flamant, G., et al. (2011). Numerical simulation of convective heat transfer between air flow and ceramic foams to optimise volumetric solar air receiver performances. *International Journal of Heat and Mass Transfer*, vol. 54, no. 7, pp. 1527–1537.

[18] Lee, H. J. (2014). The geometric-optics relation between surface slope error and reflected ray error in solar concentrators. *Solar Energy*, vol. 101, pp. 299–307.

[19] Kribus, A., Grijnevich, M., Gray, Y., et al. (2014). Parametric study of volumetric absorber performance. *Energy Procedia*, vol. 49, pp. 408–417.